Intranasal administration of Cytoglobin modifies human umbilical cord-derived mesenchymal stem cells and improves hypoxic-ischemia brain damage in neonatal rats by modulating p38 MAPK signaling-mediated apoptosis

HANHUA YANG[1,2], SHUFENG TIAN[3], LICHUN XIE[3], YUNBIN CHEN[1,4] and LIAN MA[3]

[1]Department of Pediatrics, The First Affiliated Hospital, Jinan University, Guangzhou, Guangdong 510630; [2]Department of Pediatrics, Maternal and Child Health Care Hospital, Pingshan, Shenzhen, Guangdong 518122; [3]Department of Pediatrics, Shenzhen Children's Hospital, Shenzhen, Guangdong 518038; [4]Department of Neonatology, Guangdong Women and Children Hospital, Guangzhou, Guangdong 510010, P.R. China

Received April 16, 2020; Accepted July 17, 2020

DOI: 10.3892/mmr.2020.11436

Abstract. Neonatal hypoxic-ischemic brain damage (HIBD) is a common clinical syndrome in newborns. Hypothermia is the only approved therapy for the clinical treatment; however, the therapeutic window of hypothermia is confined to 6 h after birth and even then, >40% of the infants either die or survive with various impairments, including cerebral palsy, seizure disorder and intellectual disability following hypothermic treatment. The aim of the present study was to determine whether nasal transplantation of Cytoglobin (CYGB) genetically modified human umbilical cord-derived mesenchymal stem cells (CYGB-HuMSCs) exhibited protective effects in neonatal rats with HIBD compared with those treated without genetically modified CYGB. A total of 120 neonatal Sprague-Dawley rats (postnatal day 7) were assigned to either a Sham, HIBD, HuMSCs or CYGB-HuMSCs group (n=30 rats/group). For HIBD modeling, rats underwent left carotid artery ligation and were exposed to 8% oxygen for 2.5 h. A total of 30 min after HI, HuMSCs (or CYGB-HuMSCs) labeled with enhanced-green fluorescent protein (eGFP) were intranasally administered. After modeling for 3, 14 and 29 days, five randomly selected rats were sacrificed in each group, and the expression levels of CYGB, ERK, JNK and p38 in brain tissues were determined. Nissl staining of the cortex and hippocampal Cornu Ammonis 1 area of rats in each group were compared after 3 days of modeling. TUNEL assay and immunofluorescence were performed 3 days after modeling. Long term memory in rats was assessed using a Morris-water maze 29 days after modeling. The HIBD group demonstrated significant deficiencies compared with the Sham group based on Nissl staining, TUNEL assay and the Morris-water maze test. HuMSC treated rats exhibited improvement on in all the tests, and CYGB-HuMSCs treatment resulted in further improvements. PCR and western blotting results indicated that the CYGB mRNA and protein levels were increased from day 3 to day 29 after transplantation of CYGB-HuMSCs. Furthermore, it was identified that CYGB-HuMSC transplantation suppressed p38 signaling at all experimental time points. Immunofluorescence indicated the scattered presence of HuMSCs or CYGB-HuMSCs in damaged brain tissue. No eGFP and glial fibrillary acidic protein or eGFP and neuron-specific enolase double-stained positive cells were found in the brain tissues. Therefore, CYGB-HuMSCs may serve as a gene transporter, as well as exert a neuroprotective and antiapoptotic effect in HIBD, potentially via the p38 mitogen-activated protein kinase signaling pathway.

Correspondence to: Professor Lian Ma, Department of Pediatrics, Shenzhen Children's Hospital, 17019 Yi Tian Road, Shenzhen, Guangdong 518038, P.R. China
E-mail: malian8965@sina.com

Professor Yunbin Chen, Department of Neonatology, Guangdong Women and Children Hospital, 13 West Guanyuan Road, Guangzhou, Guangdong 510010, P.R. China
E-mail: 1225990082@qq.com

Key words: cytoglobin, stem cells, intranasal administration, hypoxic-ischemic brain damage, apoptosis

Introduction

Neonatal hypoxic-ischemic brain damage (HIBD) is a common clinical syndrome in newborns caused by anoxia and reduced cerebral blood flow or temporary severance during the perinatal period (1-3). It has been reported that 2-6/1,000 newborns experience HIBD (4), and ~25% of infants who have HIBD develop neurologic sequela (5,6). Hypothermia is the only admitted therapy for treatment of neonatal HIBD in the clinic; however, the therapeutic window of hypothermia is confined to 6 h after birth, and even then, >40% of the infants either died or survive with various impairments following hypothermic treatment (7-9). Thus, alternative effective and safe therapies for treatment of HIBD are required.

Globins are hemoproteins that bind O_2 and serve an important role in the animal's respiration and oxidative energy production (10,11). However, globins may also possess other functions, such as the decomposition of nitric oxide (NO), the detoxification of reactive oxygen species (ROS) or intracellular signaling (12). Cytoglobin (CYGB), the fourth member of the vertebrate globin family of hemoproteins, is ubiquitously expressed in various tissues and organs, including the liver, kidney, brain and retina (13). CYGB may serve a cytoprotective role under hypoxic and/or ischemic conditions (14-17). Previous studies have also reported that pretreatment of CYGB-overexpression reduces HI injury and improves long term memory and athletic ability following neonatal HIBD (18). However, a safe and effective method of upregulating CYGB expression in animals remains a challenge that requires further investigation.

Previous studies have revealed that several types of cells may serve important roles in relieving HIBD (19-21). Preclinical trials on stem cells in cerebral palsy have been conducted and have reported significant improvements in acute hypoxic injury animal models (22). Mesenchymal stem cells (MSCs) are well-known for their 'immunosuppressive' properties, and thus may be important candidates for allogeneic cell therapy (23). In recent years, human umbilical cord-derived MSCs (HuMSCs) have become an alternate source of MSCs. Moreover, studies have observed that transplantation of HuMSCs at an early stage following HIBD can reduce HI injury in rats and decrease gliosis (24,25). Stem cells can also act as a gene transporter in gene therapy (26). The use of stem cells as transgenic strategies does not require integration of the therapeutic DNA into the chromosomes of the patient's cells, and instead, the transferred DNA is stabilized extrachromosomally (27). However, it has been identified that there are major risks associated with the use of integrating vectors, including retroviral vectors, arising from their potential for insertional mutagenesis, in which the vector inserts into the DNA of a cell and disrupts a functional element of that DNA (27); it has been reported that stem cell transgenic therapy can reduce this risk (28).

The aim of the present study was to investigate whether nasal transplantation of CYGB genetically modified HuMSCs (CYGB-HuMSCs) exhibited higher protective effects in neonatal rats from HIBD compared with rats treated without CYGB genetically modified HuMSCs. Additionally, the potential underlying mechanism was examined.

Materials and methods

Preparation of HuMSCs. Ethical approval was obtained from the Institutional Review Board of Maternal and Child Health Care Hospital of Shenzhen University (approval no. SZPSFY2017-06). HuMSCs were prepared as previously described (29). With the written consent of the patients, human umbilical cords from 5 patients (age range, 23-34 years old) who underwent full-term caesarian sections in the Maternal and Child Health Care Hospital (Pingshan, Shenzhen, China) from February 2018 to March 2018 were collected immediately into sterilized 50 ml tubes. After washing with PBS for 30 sec, the human umbilical cord was cut into 2-3 cm thick sections. The umbilical arteries and veins were removed, and the remaining tissue, the Wharton's jelly, was dissected into smaller fragments and transferred to 75 cm^2 flasks containing DMEM/F12 media (Gibco; Thermo Fisher Scientific, Inc.) supplemented with 10% FBS (Gibco; Thermo Fisher Scientific, Inc.), 100 μg/ml penicillin/streptomycin (Sangon Biotech Co., Ltd.), 1 g/ml amphotericin B (Gilead Sciences, Inc.), 5 ng/ml epidermal growth factor (PeproTech, Inc.) and 5 ng/ml basic fibroblast growth factor (PeproTech, Inc.). Cultures remained undisturbed for 5-7 days at 37˚C with 95% air/5% CO_2 in a humidified incubator to allow migration of cells from the explants. Subsequently, the media was replaced. After three passages, cells were harvested. Cells were observed under a Zeiss Axio Imager Z1 light inverted microscope (magnification, x100; Carl Zeiss AG).

Adenovirus-mediated transfection. Adenovirus plasmid carrying CYGB (Ad-CYGB) was purchased from Guangzhou Forevergen Technology Co., Ltd. Adenovirus plasmid carrying only enhanced green fluorescent protein (eGFP) was used as the transfection control. The transfection was performed using Lipofectamine® 2000 reagent (Invitrogen; Thermo Fisher Scientific, Inc.). HuMSCs were seeded into 12-well plates at a concentration of $2x10^5$ cells per well. After culture for 12 h, Ad-CYGB (2 μl; multiplicity of infection, 10) were added to the respective wells; the same volume of control adenovirus was added. On the second day after infection, the virus-containing medium was aspirated and replaced with fresh complete medium to continue the culture. The culture medium was replaced every 2 days thereafter for a total period of 7 days. Follow-up experiments were performed 48 h after the transfection. Cells were observed under a Zeiss Axio Imager Z1 fluorescent inverted microscope (magnification, x200; Carl Zeiss AG).

Experimental animals. Sprague-Dawley rats (age, 7 days; 64 females; 56 males; weight, 12.5-16.3 g) were obtained from the Experimental Animal Center of Shantou University Medical College. The present study was approved by the Institutional Animal Care and Use Committee of Shenzhen University (approval no. 2017-06) and strictly adhered to the ARRIVE guidelines (30). All animals were maintained in a temperature- and humidity-controlled room (temperature, 22-24˚C; humidity, 40-70%) with a 12 h light/dark cycle, and free access to food and water. Throughout the experiment, all animals were treated in accordance with the Guide for the Care and Use of Laboratory Animals in Shenzhen University, and all procedures conformed to internationally accredited guidelines and ethical regulations on animal research. Surgery was performed under isoflurane anesthesia, and all efforts were made to reduce the total number of animals used and minimize their potential suffering.

Animal groups. A total of 120 Sprague-Dawley rats were used in the present experiment. The rats were divided into four groups, with 30 rats in each group. Sham group animals received only anesthesia and exposure of the left common carotid artery, but no ligation and hypoxia operation. Animals in the HIBD, HuMSCs and CYGB-HuMSCs groups received ligation of the left common carotid artery combined with hypoxia. A total of 30 min after HIBD model preparation,

animals in the HuMSCs group and CYGB-HuMSCs group received intranasal administration of $1x10^6$ HuMSCs or CYGB-HuMSCs (3 μl), respectively. Animals in the HIBD group received only PBS (3 μl) via intranasal administration.

Establishment of an animal model of HIBD and transplantation of HuMSCs. The HIBD neonatal rat model was based on the classical Rice-Vannucci model (31). The experimental rat was deeply anesthetized via inhalation of isoflurane (3% to effect). Then, the left common carotid artery was exposed, followed by double-ligation with 5-0 silk sutures and the artery between the ligations was cut off. The wound was then sutured. The total time for surgery in each animal was ≤3 min. The body temperature of the animal was maintained at 37˚C with a radiant warmer table. After surgery, animals were allowed 1-2 h to recover from anesthesia with their mother. After recovery, animals were placed in a container with a lowered oxygen percentage (8% oxygen balanced with 92% nitrogen) and placed in a 37˚C water bath for 2.5 h to induce systemic hypoxia. Animals in the sham group only received anesthesia and exposure of the left common carotid artery. A total of 30 min after HI, $1x10^6$ cells HuMSCs or CYGB-HuMSCs (3 μl) were intranasally administered, respectively. As described previously (32), prior to the administration of HuMSCs, to increase the permeability of the nasal mucosa, nostrils were treated with 3 μl hyaluronidase (100 U; Sigma-Aldrich; Merck KGaA) in PBS. A total of 30 min later, animals were administered 3 μl HuMSCs, CYGB-HuMSCs ($1x10^6$ cells) or PBS (3 μl) twice in each nostril.

Observation. After modeling for 3, 14 and 29 days, five randomly selected rats were sacrificed via inhalation anesthesia with isoflurane (3% to effect) followed by decapitation in each group. Then, reverse transcription-quantitative (RT-q) PCR and western blotting were used to detect CYGB expression in brain tissues. Additionally, ERK, phosphorylated-(p-) ERK, JNK, p-JNK, p38 and p-p38 protein expression levels were assessed using western blotting. Nissl staining results of the cortex and hippocampal Cornu Ammonis 1 (CA1) area of rats in each group were compared after modeling for 3 days. TUNEL assays and immunofluorescence were performed on day 3 after modeling; immunofluorescence was also performed on day 14. Moreover, a Morris-Water maze experiment was used 29 days after modeling.

Nissl staining. The obtained brain specimens were fixed in 4% (w/v) formaldehyde at room temperature for 36 h, paraffin-embedded and sliced into 3-μm thick sections. The paraffin sections were deparaffinized in xylene and rehydrated in a descending ethanol series at room temperature, then, the sections were immersed in 1% toluidine blue stain at 37˚C. After 5 min, the sections were washed with water, differentiated with 1% glacial acetic acid and placed in xylene for 5 min at room temperature. Then the slices were removed from the xylene, dried and sealed with neutral gum. Samples were observed under a light microscope (Olympus BX43; Olympus Corporation) at x200 magnification.

TUNEL staining. TUNEL staining was performed on paraffin sections using an *in-situ* cell death detection kit (DeadEnd™ Fluorometric TUNEL system; Promega Corporation), according to the manufacturer's protocol. Paraffin sections were prepared and fixed as previously described for Nissl staining. Paraffin sections were dewaxed in xylene and rehydrated in a descending ethanol series at room temperature, then treated with 20 mg/l DNase proteinase K at 20-37˚C for 15 min. Subsequently, the sections were washed with PBS three times. Sections were then covered with 100 μl equilibration buffer and incubated at room temperature for 5-10 min. After removing the balance solution, 50 μl rTdT incubation buffer was added and the sections covered with plastic coverslips to incubate at 37˚C for 60 min. Sections were then immersed in 2X saline sodium citrate in a dyeing tank at room temperature for 15 min. To stop the reactions, sections were washed twice with PBS. Subsequently, sections were stained with 1X Hoechst nuclear stain at 37˚C for 15 min and mounted with neutral gum. Samples were observed under a Zeiss Axio Imager Z1 fluorescent microscope (magnification, x200; Carl Zeiss AG) in three randomly selected fields of view. Image-Pro-Plus software (version 6.0; Media Cybernetics, Inc.) was used to perform the semi-quantitative analysis of the apoptotic cells.

Immunofluorescence. Paraffin sections were prepared and fixed as previously described for Nissl staining. The paraffin sections were deparaffinized in xylene and rehydrated using a descending ethanol series at room temperature. Then, the sections were permeabilized with 0.1% Triton X-100 at room temperature for 10 min. Sections were blocked with normal goat blocking serum (Abbkine Scientific Co., Ltd.) at a volume fraction of 3% at room temperature for 1 h. After washing three times with PBS for 2 min/time, sections were treated overnight with primary antibody at 4˚C. The primary antibodies used were glial fibrillary acidic protein (GFAP; Cell Signaling Technology, Inc.; cat. no. 80788S; 1:50) and neuron-specific enolase (NSE; ProteinTech Group, Inc.; cat. no. 10149-1-AP; 1:50). The sections were rinsed twice with PBS and then incubated with the secondary Alexa Fluor 555 antibody (Abcam; cat. no. ab150074; 1:200) for 1 h at room temperature in the dark. Samples were observed under a Zeiss Axio Imager Z1 fluorescent microscope (magnification, x200; Carl Zeiss AG).

RT-qPCR. After HI modeling for 3, 14 or 29 days, rats from different groups were anesthetized and decapitated. Samples of injured brain tissues were collected rapidly and total RNA was prepared from samples collected using TRIzol® reagent (Invitrogen; Thermo Fisher Scientific, Inc.) as previously described (33). Total RNA (2 μg) was reverse transcribed using M-MLV reverse transcriptase (Promega Corporation). In a sterile RNase-free microcentrifuge tube, 2 μg total RNA and 1 μg primer in a total volume of 15 μl in water were added. The tube was heated tube to 70˚C for 5 min. Then, the tube was cooled immediately on ice and centrifuged (500 x g; 4˚C; 1 min) briefly to collect the solution at the bottom of the tube. In total, 5 μl 5X buffer, 6.25 μl 2 mM dNTP, 1 μl M-MLV and 12.75 μl RNase-free water were added to the tube, which was mix gently and incubated for 60 min at 42˚C. cDNA expression levels were determined via qPCR using specific primers and GoTaq® qPCR Master mix (Promega Corporation) in a StepOne Plus amplifier (Bio-Rad Laboratories, Inc.). The thermocycling protocol was as follows: Initial denaturation at 95˚C

for 120 sec; followed by 40 cycles at 95˚C for 15 sec, 60˚C for 30 sec and 72˚C for 45 sec, and then a final elongation at 72˚C for 10 min. Data were quantified using the $2^{-\Delta\Delta Cq}$ method (34). The primers used were as follows: CYGB (NM_134268.5; product length, 152 bp) forward, 5'-TTGCCAGTGACTTCC CACC-3' and reverse 5'-CCCGAAGAGGGCAGTGTG-3'; and GAPDH (NM_001289745.3; product length, 185 bp) forward, 5'-GAGTCAACGGATTTGGTCG-3' and reverse 5'-GAG TCAACGGATTTGGTCGT-3'.

Western blotting. Brain tissues collected simultaneously for the qPCR experiments were homogenized in ice-cold RIPA lysis buffer (Beyotime Institute of Biotechnology), and the protein concentrations were measured using a bicinchoninic acid protein assay kit (Beyotime Institute of Biotechnology). A total of 40 μg total protein per lane was loaded on a 12% SDS-gel, resolved using SDS-PAGE and transferred to a PVDF membrane (EMD Millipore). The membrane was blocked with TBS-Tween (20 mM Tris; pH 7.6; 135 mM NaCl; 0.05% Tween) containing 5% non-fat dry milk overnight at 4˚C, washed with 1X TBS-0.1% Tween-20 and then incubated at 4˚C with primary antibodies in blocking solution. The following primary antibodies were used: GAPDH (1:10,000; cat. no. 10494-1-AP; ProteinTech Group, Inc.), CYGB (1:1,000; cat. no. 13317-1-AP; ProteinTech Group, Inc.), p-p38 (1:1,000; cat. no. 4511S; Cell Signaling Technology, Inc.), p38 (1:1,000; cat. no. 8690S; Cell Signaling Technology, Inc.), p-ERK (1:1,000; cat. no. 4370; Cell Signaling Technology, Inc.), ERK (1:1,000; cat. no. 9102; Cell Signaling Technology, Inc.), p-JNK (1:1,000; cat. no. 4668; Cell Signaling Technology, Inc.) and JNK (1:1,000; cat. no. 9252; Cell Signaling Technology, Inc.). After washing the membrane four times with TBS-Tween, the horseradish peroxidase-labeled secondary goat anti-rabbit IgG antibody (1:8,000; cat. no. RS0002; Immunoway; Suzhou Ruiying Biotechnology Co., Ltd.), was added and incubated for 2 h at room temperature, and then washed again. Protein bands were visualized using an ECL Plus chemiluminescence kit (Guangzhou Forevergen Technology Co., Ltd.). ImageJ software version 1.52 h (National Institutes of Health) was used to perform the densitometric analysis.

Morris-Water maze test. The water maze was composed of a cylindrical pool and a platform. The height of the pool was 70 cm and the diameter was 80 cm. The diameter of the platform was 8 cm. Over the pool, there was a digital camera connected to the computer. The pool was filled with water until the surface of the water was ~0.5 cm above the surface of the platform, the water temperature was controlled at 22.0±0.5˚C. A specific point on the pool was used as the point of entry for rats. The platform was placed in the third quadrant, and the position of the platform was unchanged throughout the entire experimental process. Training twice a day started 4 days prior to the formal experiment; rats were placed in the water from the four quadrants. If the animal found the platform within 120 sec, it was left on the platform for 20 sec. If the animal did not find the platform, it was placed on the platform and left for 20 sec. On the second day after the training finished, experiments were performed to record the time and the path length (PL) from the point of entry to the platform in 120 sec.

Statistical analysis. Statistical analysis was performed using GraphPad Prism version 8 (GraphPad Software, Inc.). Continuous experimental data are presented as the mean ± standard deviation of ≥3 experimental repeats. A one-way ANOVA followed by Tukey's of Bonferroni post hoc test was used to compare the differences between multiple groups. $P<0.05$ was considered to indicate a statistically significant difference.

Results

Morphology of cultured HuMSCs and transfection. After 5-7 days of culture, fibroblast-like cells migrated out from the surrounding tissues. Primary HuMSCs were passaged when they were cultured for 10-14 days and the cells reached 80% confluence. In the 3rd generation, cells had a stable fibroblast-like morphology (Fig. 1A). The results of eGFP immunofluorescence analysis demonstrated that the adenovirus plasmid transfection efficiency was ~80% (Fig. 1B and C). Furthermore, RT-qPCR results suggested that the transfected CYGB gene was efficiently expressed in HuMSCs (Fig. 1D and E).

Observation of histological changes in the brain using Nissl staining after modeling for 3 days. Neuronal cell loss in both the cerebral cortex and hippocampus was observed via Nissl staining after modeling for 3 days. HI markedly reduced the number of cells and resulted in irregularly arranged and smaller neurons in the brain 3 days after HI compared with the sham group (Fig. 2). However, in the HuMSCs group, nerve cells were regularly arranged and survival numbers were notably increased compared with the HI group (Fig. 2). Furthermore, high numbers of Nissl-stained cells were observed in the CYGB-HuMSCs group compared with the HuMSCs group (Fig. 2).

TUNEL staining. To determine whether HuMSCs and CYGB-HuMSCs transplantation prevented apoptosis at the acute stage of neonatal HI injury, TUNEL staining of tissue sections was performed after 3 days of modelling (Fig. 3A and B). Significantly fewer apoptotic cells were observed in the HuMSCs group compared with the HI groups ($P<0.01$), and the number of apoptotic cells was significantly lower in the CYGB-HuMSCs group compared with the HuMSCs groups (Fig. 3A-C).

Immunofluorescence. To assess whether HuMSCs or CYGB-HuMSCs underwent cell replacement via differentiation into neuron-like cells, immunofluorescence co-localization analysis was performed 3 and 14 days after HI. It was identified that HuMSCs or CYGB-HuMSCs were present and scattered in the damaged brain tissue (Fig. 4). Moreover, no eGFP and GFAP or EGFP and NSE double-stained positive cells were observed and no substantial differences were observed between 3 and 14 days.

Expression of CYGB after transplantation of HuMSCs. To investigative the mRNA and protein expression levels of CYGB following CYGB-HuMSCs transplantation, RT-qPCR and western blotting were performed on samples collected from all groups following HI modeling for 3, 14 and 29 days.

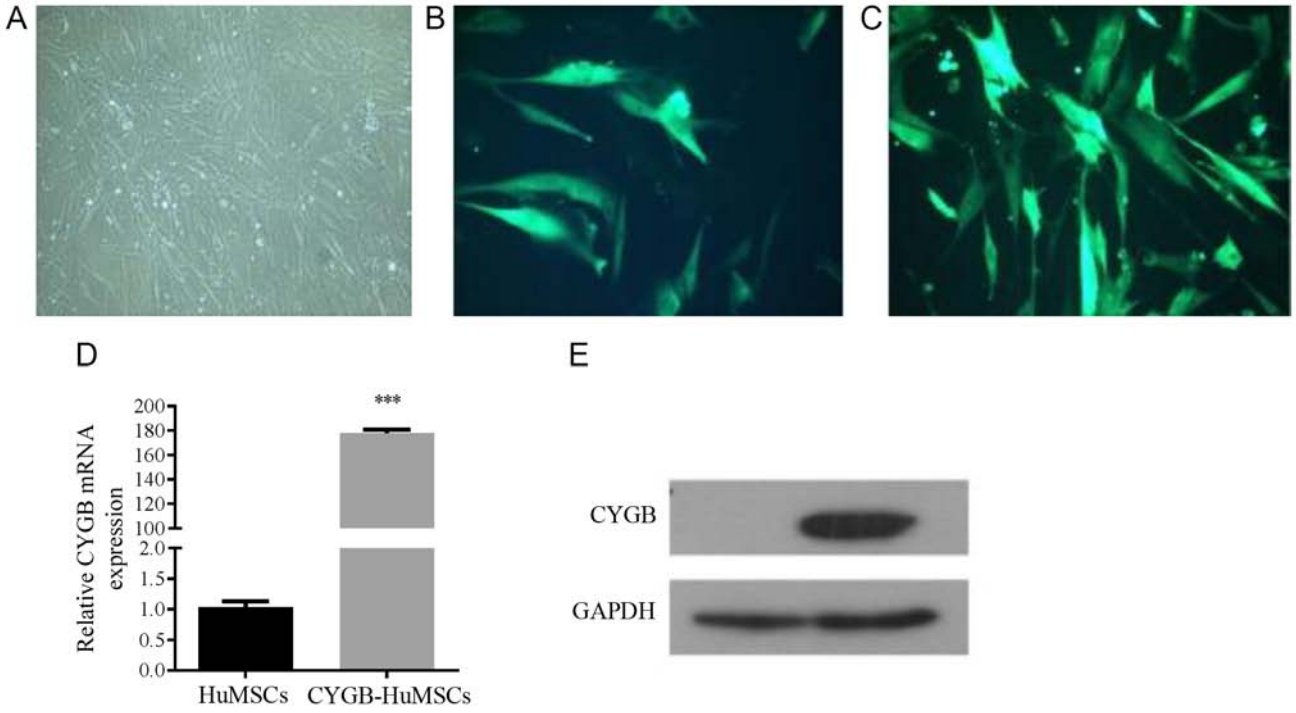

Figure 1. Morphology of cultured HuMSCs. (A) HuMSCs after the third passage exhibited a fibroblast-like morphology. Magnification, x100. eGFP fluorescence of HuMSCs transfected with (B) Ad-eGFP or (C) Ad-CYGB. Magnification, x200. (D) mRNA and (E) protein expression levels of CYGB in HuMSCs transfected with Ad-eGFP or Ad-CYGB after 48 h. ***P<0.001 vs. HuMSC. HuMSC, human umbilical cord-derived mesenchymal stem cells; eGFP, enhanced green fluorescent protein; Ad-eGFP, Adenovirus plasmid carrying eGFP; CYGB, Cytoglobin.

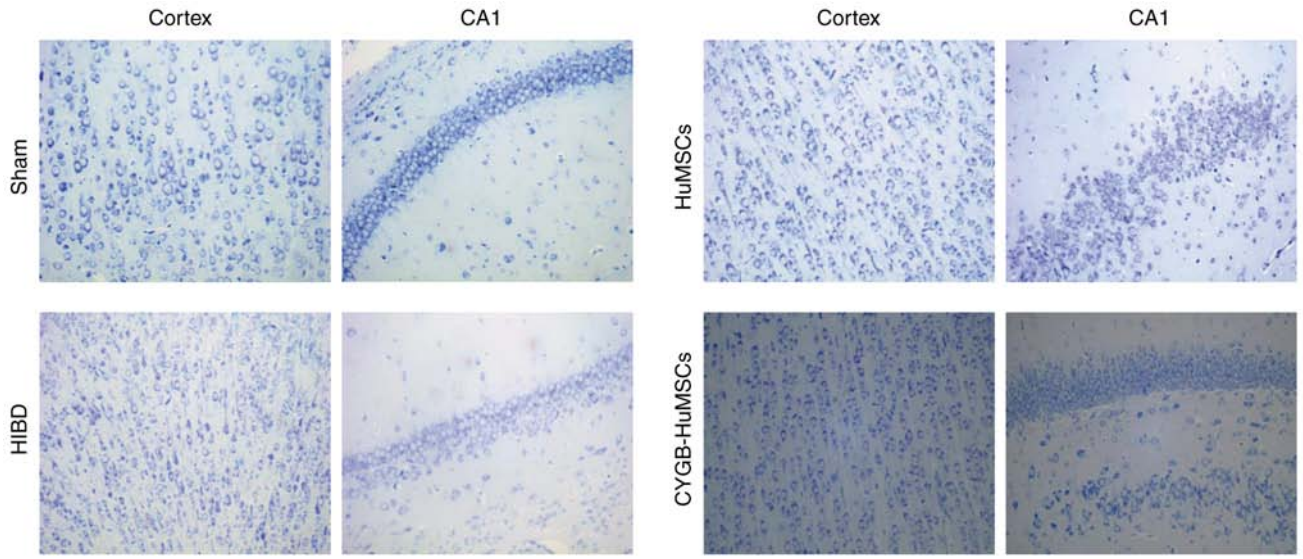

Figure 2. Morphology of neuronal cells in both the cortex and hippocampus CA1 area 3 days after HI and in the sham group. Magnification, x200. HI, hypoxia-ischemia injury; CA, Cornu Ammonis. HIBD, hypoxic-ischemia brain damage; HuMSC, human umbilical cord-derived mesenchymal stem cells; CYGB, Cytoglobin.

RT-qPCR results demonstrated that CYGB mRNA expression was significantly increased in the CYGB-HuMSCs group compared with the HIBD and HuMSCs groups (Fig. 5C) at all experimental time points. CYGB mRNA expression was significantly increased in the HuMSCs group compared with the HIBD group, but significantly decreased compared with the CYGB-HuMSC group at 14 and 29 days (Fig. 5C). Western blotting results identified that CYGB protein expression was also increased in the CYGB-HuMSCs group compared with the HIBD and HuMSCs groups. At all experimental time points, CYGB protein expression was also increased in the HuMSCs group compared with the HIBD group, while decreased compared with the CYGB-HuMSCs group. The expression levels of CYGB protein in both the HuMSCs and CYGB-HuMSCs groups gradually declined from 3 to 29 days (Fig. 5A and B).

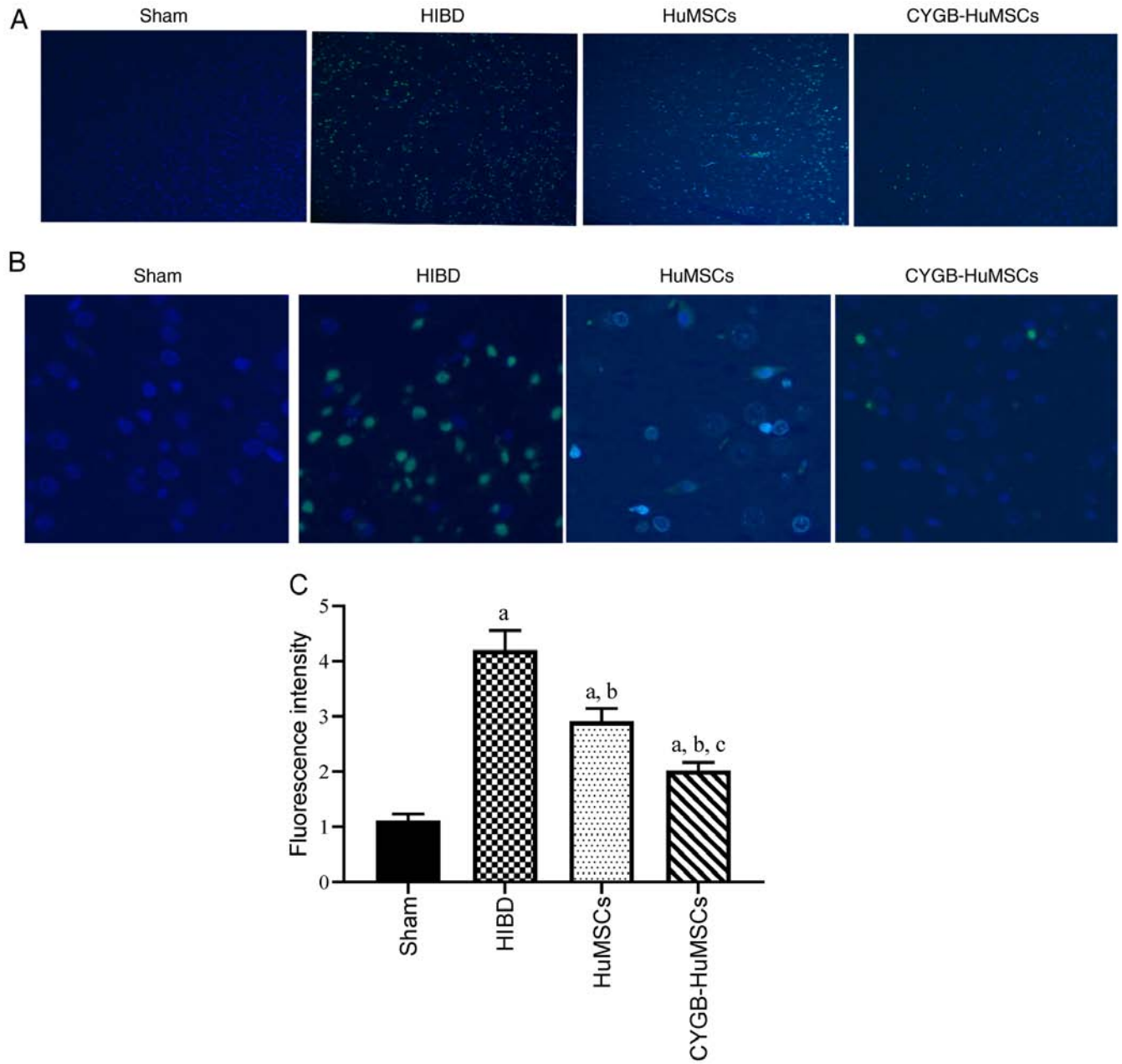

Figure 3. Levels of neural cell apoptosis 3 days after HI. (A) TUNEL staining was performed to evaluate neural cell apoptosis at an acute stage of neonatal HI injury and in the sham group (n=5). Magnification, x100. (B) TUNEL staining on day 3 after HI and in the sham group. Magnification, x200. (C) Significantly fewer apoptotic cells were observed in the HuMSCs group compared with the HIBD group. The number of apoptotic cells was significantly lower in the CYGB-HuMSCs group compared with the HuMSCs groups. [a]P<0.01 vs. Sham group at the same time; [b]P<0.01 vs. HIBD group at the same time; [c]P<0.01 vs. HuMSCs group at the same time. HI, hypoxia-ischemia injury; HuMSC, human umbilical cord-derived mesenchymal stem cells; CYGB, Cytoglobin; HIBD, hypoxic-ischemia brain damage.

Morris-Water maze test. The Morris-Water maze experiment was performed 29 days after HI to evaluate long term learning and memory, which is dependent on the function of the hippocampus and cortex (18). The results indicated a longer escape latency (EL) in the HIBD group compared with the sham group. EL in the HuMSCs group was significantly shorter compared with the HIBD group, and in the CYGB-HuMSCs group, EL was shorter compared with the HuMSCs group (Fig. 6A). The PL was also recorded. PL was longer in the HIBD group compared with the sham group (Fig. 6B). Furthermore, HuMSCs transplantation significantly reduced PL compared with the HIBD rats, and CYGB-HuMSCs transplantation resulted in further reduced PL values compared with HuMSCs transplantation. These results indicated a long-term neuroprotective effect of either HuMSCs or CYGB-HuMSCs on HIBD.

CYGB-HuMSCs treatment modulates the p38 pathway. As demonstrated by the western blotting results (Fig. 7), compared with the Sham group, the ratio of p-p38/p38 was significantly increased in the HIBD group after HI modeling for 3, 14 and 29 days (Fig. 7A-C), suggesting that hypoxia and oxidative stress mediated the stimulation of p38 signaling. HuMSCs treatment significantly reduced the ratio of p-p38/p38 after HI modeling for 3 and 29 days (Fig. 7A and C). The ratio of p-p38/p38 at all

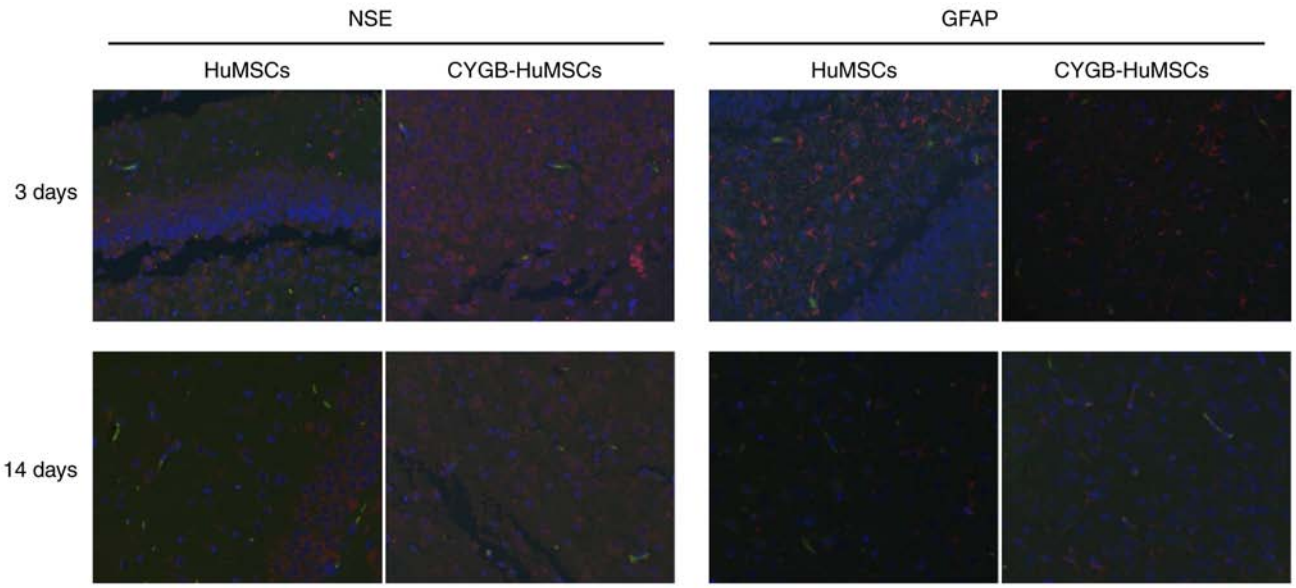

Figure 4. Distribution, survival and differentiation of HuMSCs or CYGB-HuMSCs 3 and 14 days after HI. HuMSCs or CYGB-HuMSCs were scattered in the damaged brain tissue. No eGFP and GFAP or eGFP and NSE double stained positive cells were observed. Magnification, x100. HuMSC, human umbilical cord-derived mesenchymal stem cells; HI, hypoxia-ischemia injury; CYGB, Cytoglobin; eGFP, enhanced GFP; GFAP, glial fibrillary acidic protein; NSE, neuron-specific enolase.

experimental time points in the CYGB-HuMSCs group was significantly lower compared with the HuMSCs group (Fig. 7). Moreover, the ratio of p-p38/p38 in the CYGB-HuMSCs group was significantly lower compared with the sham group on day 3 after transplantation of CYGB-HuMSCs (Fig. 7A).

The ratio of p-JNK/JNK in the HIBD group was significantly increased compared with the Sham group after HI modeling for 14 and 29 days (Fig. 7B and C). On day 14 after HI modeling, compared with the HIBD group, the ratio of p-JNK/JNK was decreased in the HuMSCs group and CYGB-HuMSCs group; however, the ratio in the CYGB-HuMSCs group remained higher than the HuMSCs group (Fig. 7B). On day 29 after HI modeling, there were no significant differences in the ratio of p-JNK/JNK between the HIBD group and HuMCSs or CYGB-HuMSCs groups, but the ratio in the CYGB-HuMSCs group was lower compared with the HuMSCs group (Fig. 7C).

The ratio of p-ERK/ERK in the HIBD group was significantly decreased compared with the Sham group after HI modeling for 3 days, while increased at day 14 after HI modeling (Fig. 7A and B). On days 3 and 29 after HI modeling, compared with the HIBD group, the ratio of p-ERK/ERK was increased in the HuMSCs group and CYGB-HuMSCs group (Fig. 7A and C). On day 14 after HI modeling, compared with the HIBD group, the ratio of p-ERK/ERK was decreased in the HuMSCs group, while increased in the CYGB-HuMSCs group (Fig. 7B).

Discussion

HIBD is a significant threat to neonatal health, which results in disability and mortality in infants and children (5,6). Despite an increase in the number of studies that have been performed to investigate the pathogenesis of HIBD, hypothermia and systemic supportive treatment are the primary therapeutic options for HIBD (35). To the best of our knowledge, the present study was the first to demonstrate that intranasal transplantation of CYGB-HuMSCs exhibited neuroprotective and antiapoptotic effects in HIBD. In a rat model of HIBD, intranasal administration of both HuMSCs and CYGB-HuMSCs resulted in reduced severity of histological and functional deficits. In addition, the reduction in the CYGB-HuMSCs group was more prominent compared with the HuMSCs group.

CYGB has been extensively studied in the past 15 years (13), following its discovery. Different from hemoglobin, CYGB is found outside of red blood cells and is classified as a non-erythroid globin, similar to other globins, such as neuroglobin and myoglobin (36). The potential functions of these non-erythroid globins are associated with tissue and cell protection under hypoxic conditions, ischemic conditions and during oxidative stress (37). Due to the structure of the hemeglobin, CYGB can reversibly bind to oxygen and other small molecules (38). The ability of CYGB to store and sense oxygen, as well as its involvement in nitrite and NO metabolism, are being increasingly studied and understood (39,40). It has been reported that, similar to other hemoglobins, CYGB can scavenge ROS and NO, as well as produce NO from nitrite, thus reducing oxidative stress and protecting organs and cells (41-44). Our previous study revealed that pretreatment of CYGB-overexpression reduced neonatal rat HI injury, as well as improved long term memory and athletic ability following neonatal HI (18). However, whether overexpression of CYGB serves a protective role in neurons following HIBD has not been previously studied, and there is no established means of introducing the CYGB gene safely into living animals.

In the present study, the effect of transplantation of CYGB-HuMSCs in an HIBD rats model was determined, and was developed based the application of stem cells for treatment of various brain diseases and our previous study (18). The current results suggested that CYGB-HuMSCs reduced

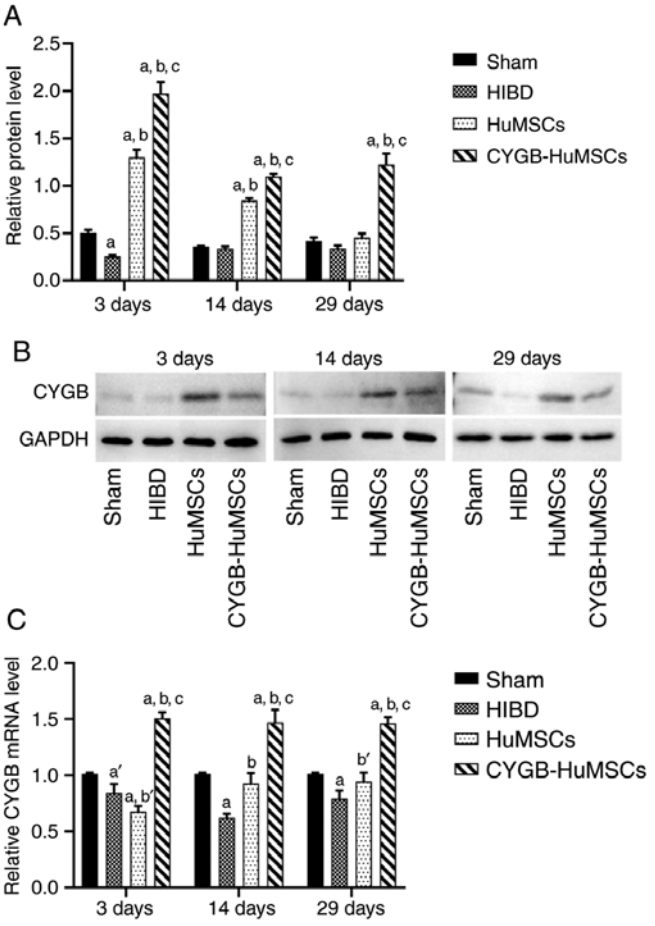

Figure 5. Expression of CYGB in all groups after HI modeling for 3, 14 and 29 days (n=5 per group). (A) Expression of CYGB protein was assessed using (B) western blotting. GAPDH was used as the internal control. (C) mRNA expression of CYGB mRNA was determined using reverse transcription-quantitative PCR. The results demonstrated that both the protein and mRNA expression levels of CYGB were increased in the CYGB-HuMSCs group compared with the HIBD and HuMSCs groups. [a]P<0.01 vs. Sham group at the same time; [b]P<0.01 vs. HIBD group at the same time; [c]P<0.01 vs. HuMSCs group at the same time; [a]P<0.05 vs. Sham group at the same time; [b]P<0.05 vs. HIBD group at the same time. HI, hypoxia-ischemia injury; CYGB, Cytoglobin; HuMSC, human umbilical cord-derived mesenchymal stem cells; HIBD, hypoxic-ischemia brain damage.

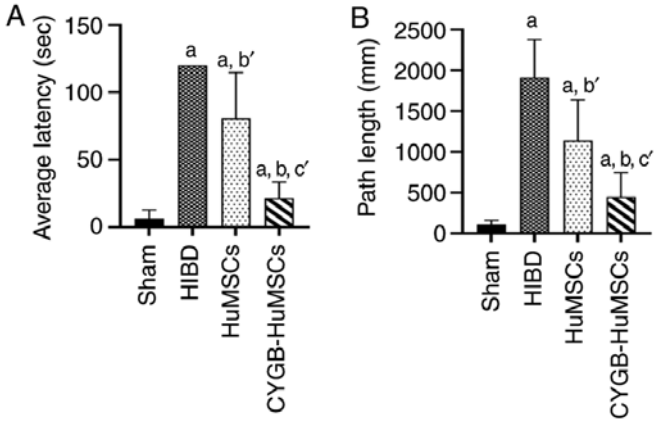

Figure 6. Morris-Water maze experiments 29 days after HI (n=5 per group). (A) EL values of the HI group were longer compared with the sham group. EL values in the HuMSCs group was significantly shorter compared with the HI group, and the EL values in the CYGB-HuMSCs group were shorter compared with the HuMSCs group. (B) PL values were longer in the HI compared with the sham group. In the HuMSCs group, PL was shorter compared with the HI group, and the PL value in the CYGB-HuMSCs group was also shorter compared with the HuMSCs group. [a]P<0.01 vs. Sham group at the same time; [b]P<0.01 vs. HIBD group at the same time; [c]P<0.01 vs. HuMSCs group at the same time; [b]P<0.05 vs. HIBD group at the same time; [c]P<0.05 vs. HuMSCs group at the same time. HI, hypoxia-ischemia injury; CYGB, Cytoglobin; HuMSC, human umbilical cord-derived mesenchymal stem cells; EL, escape latency; PL, path length; HIBD, hypoxic-ischemia brain damage.

neuron cell apoptosis caused by HIBD. The improvement in long term neurological function 29 days after HIBD further demonstrated the neuroprotective effect of CYGB-HuMSCs transplantation. HuMSCs also exhibited a neuroprotective and antiapoptotic effect in HIBD, but the CYGB-HuMSCs exhibited more prominent neuroprotective effects. In addition, RT-qPCR and western blotting results identified that CYGB mRNA and protein expression levels were increased from day 3 to day 29 after transplantation of CYGB-HuMSCs. Thus, it was suggested that CYGB functions as an endogenous neuroprotective protein, and that CYGB-HuMSCs may act as a gene transfer vector for CYGB, allowing CYGB and HuMSCs to work together to improve the neuroprotective effects. Therefore, these results highlight a novel approach for treatment of neonatal HIBD.

Previous studies have shown that HuMSCs do not undergo cell replacement via differentiation into neuron-like cells, but rather exert neuroprotective effects (45,46). In the present study, HuMSCs or CYGB-HuMSCs administered via nasal transplantation did not differentiate into cells expressing neural or glial cell marker proteins; a result that is similar to previous studies (45,46). Therefore, it was speculated that the neuroprotective effects of HuMSCs may be achieved via the action of exosomes to promote endogenous repair of nerve cells (47-49). Proteins secreted by MSCs can promote the repair of damaged tissues via a variety of mechanisms, including prevention of apoptosis, regulation of inflammatory responses and promotion of endogenous repair mechanisms, such as angiogenesis and neurogenesis, rather than cell replacement (48). In a HIBD animal model, MSCs provide a suitable environment, including increasing the local levels of brain-derived neurotrophic factor, basic fibroblast growth factor, neurotrophic factor and nerve growth factor, whilst downregulating the expression of proinflammatory cytokines, such as IL-1 and IL-6, which may also contribute to the repair of nerve cells (47,50). Previous studies have reported that CYGB serves a neuroprotective role by reducing cerebral infarctions and apoptosis caused by oxidative stress *in vivo*, and also revealed that hypoxia inducible factor-1α/CYGB/vascular endothelial growth factor signaling may serve an important role in the CYGB-mediated antioxidant mechanism (18). Therefore, it was hypothesized that the neuroprotective effects of CYGB-HuMSCs is not via cell replacement, but via the various cytokines secreted by HuMSCs and the antioxidant effects of overexpression of CYGB transfected into animals by HuMSCs.

The p38 mitogen-activated protein kinase (MAPK) signaling pathway allows cells to interpret a wide range of external signals and respond appropriately by generating a plethora of different biological effects (51). It has been revealed that p38 MAPK is a mediator of hypoxia-induced

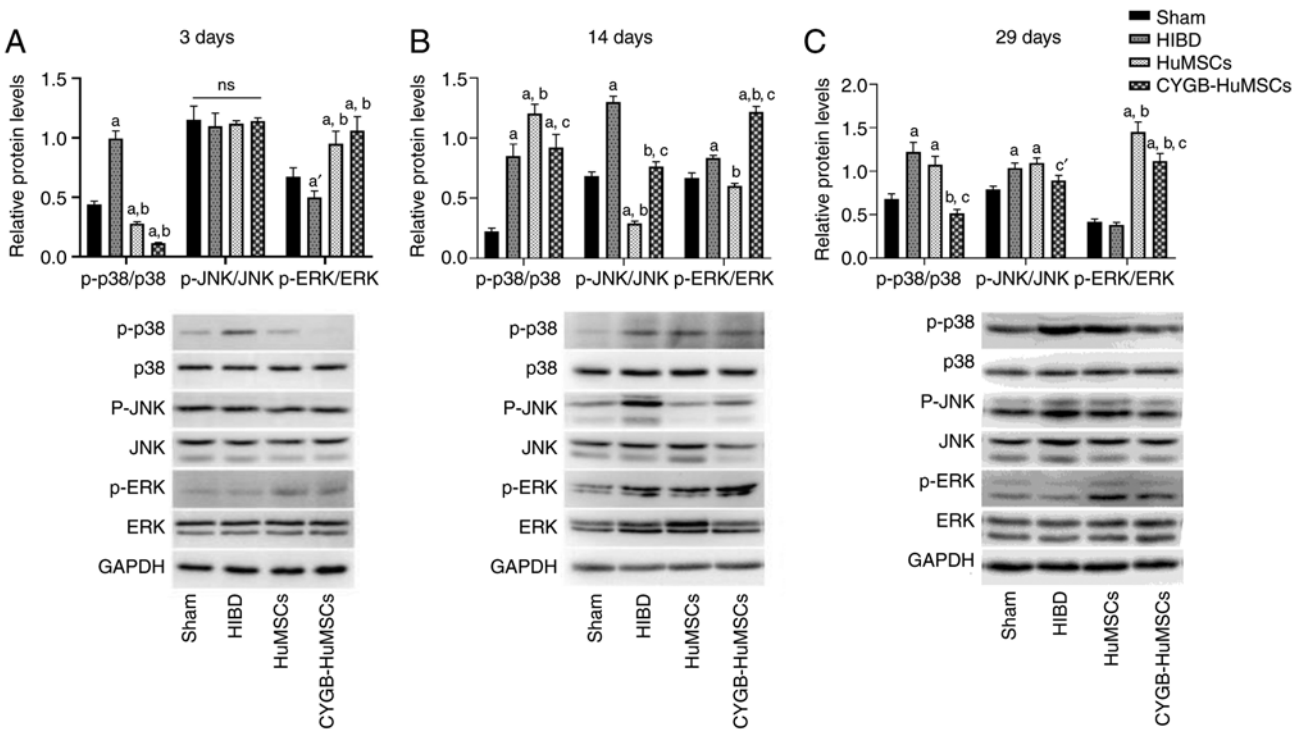

Figure 7. Expression levels of p-p38, p38, ERK, p-ERK, JNK and p-JNK after HI modeling for 3, 14 and 29 days (n=5 per group). GAPDH was used as the internal control. (A-C) The ratio of p-p38/p38 was significantly increased in the HIBD group after HI modeling for 3, 14 and 29 days. (A and C) The ratio of p-p38/p38 after HI modeling for 3 and 29 days in the HuMSCs group was decreased. (A-C) The ratio of p-p38/p38 at all experimental time points in the CYGB-HuMSCs group was significantly lower compared with the HuMSCs group. (B and C) The ratio of p-JNK/JNK in the HIBD group was significantly increased compared with the Sham group after HI modeling for 14 and 29 days. (B) On day 14 after HI modeling, compared with the HIBD group, the ratio of p-JNK/JNK was decreased in the HuMSCs and CYGB-HuMSCs groups, but those in the CYGB-HuMSCs group remained higher than the HuMSCs group. (C) On day 29 after HI modeling, there were no differences in the ratio of p-JNK/JNK between the HIBD group and the HuMCSs or CYgB-HuMSCs groups, but the ratio in the CYGB-HuMSCs group was significantly lower compared with the HuMSCs group. (A, B) The ratio of p-ERK/ERK in the HIBD group was significantly decreased compared with the Sham group after HI modeling for 3 days, while increased at day 14 after HI modeling. (A and C) On days 3 and 29 after HI modeling, compared with the HIBD group, the ratio of p-ERK/ERK was increased in the HuMSCs and CYGB-HuMSCs groups. (B) On day 14 after HI modeling, compared with the HIBD group, the ratio of p-ERK/ERK was decreased in the HuMSCs group, while increased in the CYGB-HuMSCs group. aP<0.01 vs. Sham group at the same time; bP<0.01 vs. HIBD group at the same time; cP<0.01 vs. HuMSCs group at the same time; a'P<0.05 vs. Sham group at the same time; c'P<0.05 vs. HuMSCs group at the same time; ns, no significant difference vs. other groups. p-, phosphorylated; HI, hypoxia-ischemia injury; CYGB, Cytoglobin; HuMSC, human umbilical cord-derived mesenchymal stem cells; HIBD, hypoxic-ischemia brain damage.

cerebrovascular inflammation (52). The p38 MAPK signaling pathway enhances the production of a range of proinflammatory cytokines, including IL-β, TNF-α and IL-8 (53,54). Moreover, p38 MAPK has been suggested to be involved in the context of ischemia-induced stress in the brain (55). For example, p38 MAPK inhibits the hypoxia response pathway via EGL-9 in neurons (56). The p38 MAPK can also function as a mediator of ROS-mediated signaling, and either activate or suppress cell cycle progression, depending on the activation stimulus (57). Proteomic and biochemical analyses further demonstrated that p38 MAPK signaling mediates cell apoptosis (58), while *in vitro* studies have shown that overexpression of CYGB suppressed p38 expression and protected glomerular mesangial cells from oxidative stress (59).

In the present study, the ratio of p-p38/p38 was significantly increased in the HIBD group. However, HuMSCs supplementation protected against neuron cell apoptosis as demonstrated by the decreased ratio of p-p38/p38. In addition, the CYGB-HuMSCs group had an improved antiapoptotic effect accompanied with a greater degree of decreased p38 expression compared with the HuMSCs group. The present results also suggested that the CYGB-HuMSCs group had significantly downregulated phosphorylation levels of p38, which was accompanied with a significantly increased expression level of CYGB, compared with the sham group on day 3. Thus, it was indicated that exogenous CYGB may modulate p38 expression. The current results highlight the involvement of p38 MAPK signaling in HIBD, as well as suggesting that CYGB-HuMSCs treatment may protect animals from HIBD by avoiding activation of the p38 MAPK signaling pathway.

In conclusion, to the best of our knowledge, the present study was the first to demonstrate that intranasal transplantation of CYGB-HuMSCs can serve as a gene transporter, and that it exerts neuroprotective and antiapoptotic effects in HIBD. Additionally, it was identified that CYGB-HuMSCs may exert its protective properties via the p38 MAPK pathway. The results of the current study demonstrate a novel therapeutic approach for treatment of HIBD. However, further investigation is required to identify the mechanism via which CYGB-HuMSCs contributes to the molecular pathogenesis of HIBD.

Acknowledgements

Not applicable.

Funding

The present study was supported by the Science and Technology Project from the Science Technology and Innovation Committee of Shenzhen Municipality (grant no. JCYJ20160429141742207), the National Natural Science Foundation of China (grant nos. 81671525 and 81070478) and the Sanming Project of Medicine in Shenzhen (grant no. SZSM201512033).

Availability of data and materials

The datasets used and/or analyzed during the present study are available from the corresponding author on reasonable request.

Authors' contributions

SFT, YBC and HHY designed the study and performed the experiments. HHY, LM and LCX acquired the data. SFT and HHY analyzed the data. HHY, YBC and LM prepared the manuscript. All authors read and approved the final manuscript.

Ethics approval and consent to participate

This study was approved by the Ethics Committees of Maternal and Child Health Care Hospital of Shenzhen University (Guangdong, China), and of the Institutional Animal Care and Use Committee of Shenzhen University (Guangdong, China). Written informed consent was obtained from the maternal donors and/or guardians.

Patient consent for publication

Not applicable.

Competing interests

The authors declare that they have no competing interests.

References

1. Novak CM, Ozen M and Burd I: Perinatal brain injury: Mechanisms, prevention, and outcomes. Clin Perinatol 45: 357-375, 2018.
2. du Plessis AJ and Volpe JJ: Perinatal brain injury in the preterm and term newborn. Curr Opin Neurol 15: 151-157, 2002.
3. Triulzi F, Parazzini C and Righini A: Patterns of damage in the mature neonatal brain. Pediatr Radiol 36: 608-620, 2006.
4. Gale C, Statnikov Y, Jawad S, Uthaya SN and Modi N; Brain Injuries expert working group: Neonatal brain injuries in England: Population-based incidence derived from routinely recorded clinical data held in the National Neonatal Research Database. Arch Dis Child Fetal Neonatal Ed 103: 301-306, 2018.
5. Bass JL, Corwin M, Gozal D, Moore C, Nishida H, Parker S, Schonwald A, Wilker RE, Stehle S and Kinane TB: The effect of chronic or intermittent hypoxia on cognition in childhood: A review of the evidence. Pediatrics 114: 805-816, 2004.
6. Yildiz EP, Ekici B and Tatli B: Neonatal hypoxic ischemic encephalopathy: An update on disease pathogenesis and treatment. Expert Rev Neurother 17: 449-459, 2017.
7. Chiang MC, Jong YJ and Lin CH: Therapeutic hypothermia for neonates with hypoxic ischemic encephalopathy. Pediatr Neonatol 58: 475-483, 2017.
8. Srinivasakumar P, Zempel J, Wallendorf M, Lawrence R, Inder T and Mathur A: Therapeutic hypothermia in neonatal hypoxic ischemic encephalopathy: Electrographic seizures and magnetic resonance imaging evidence of injury. J Pediatr 163: 465-470, 2013.
9. Ma H, Sinha B, Pandya RS, Lin N, Popp AJ, Li J, Yao J and Wang X: Therapeutic hypothermia as a neuroprotective strategy in neonatal hypoxic-ischemic brain injury and traumatic brain injury. Curr Mol Med 12: 1282-1296, 2012.
10. Pesce A, Bolognesi M, Bocedi A, Ascenzi P, Dewilde S, Moens L, Hankeln T and Burmester T: Neuroglobin and cytoglobin. Fresh blood for the vertebrate globin family. EMBO Rep 3: 1146-1151, 2002.
11. Gell DA: Structure and function of haemoglobins. Blood Cells Mol Dis 70: 13-42, 2018.
12. Burmester T and Hankeln T: Function and evolution of vertebrate globins. Acta Physiol (Oxf) 211: 501-514, 2014.
13. Trent JT III and Hargrove MS: A ubiquitously expressed human hexacoordinate hemoglobin. J Biol Chem 277: 19538-19545, 2002.
14. Stagner JI, Parthasarathy SN, Wyler K and Parthasarathy RN: Protection from ischemic cell death by the induction of cytoglobin. Transplant Proc 37: 3452-3453, 2005.
15. Hankeln T, Ebner B, Fuchs C, Gerlach F, Haberkamp M, Laufs TL, Roesner A, Schmidt M, Weich B, Wystub S, *et al*: Neuroglobin and cytoglobin in search of their role in the vertebrate globin family. J Inorg Biochem 99: 110-119, 2005.
16. Avivi A, Gerlach F, Joel A, Reuss S, Burmester T, Nevo E and Hankeln T: Neuroglobin, cytoglobin, and myoglobin contribute to hypoxia adaptation of the subterranean mole rat Spalax. Proc Natl Acad Sci USA 107: 21570-21575, 2010.
17. Singh S, Manda SM, Sikder D, Birrer MJ, Rothermel BA, Garry DJ and Mammen PP: Calcineurin activates cytoglobin transcription in hypoxic myocytes. J Biol Chem 284: 10409-10421, 2009.
18. Tian SF, Yang HH, Xiao DP, Huang YJ, He GY, Ma HR, Xia F and Shi XC: Mechanisms of neuroprotection from hypoxia-ischemia (HI) brain injury by up-regulation of cytoglobin (CYGB) in a neonatal rat model. J Biol Chem 288: 15988-16003, 2013.
19. Li Y and Chopp M: Marrow stromal cell transplantation in stroke and traumatic brain injury. Neurosci Lett 456: 120-123, 2009.
20. Zhao L, Johnson T and Liu D: Therapeutic angiogenesis of adipose-derived stem cells for ischemic diseases. Stem Cell Res Ther 8: 125, 2017.
21. Park WS, Sung SI, Ahn SY, Yoo HS, Sung DK, Im GH, Choi SJ and Chang YS: Hypothermia augments neuroprotective activity of mesenchymal stem cells for neonatal hypoxic-ischemic encephalopathy. PLoS One 10: e0120893, 2015.
22. Gonzales-Portillo GS, Reyes S, Aguirre D, Pabon MM and Borlongan CV: Stem cell therapy for neonatal hypoxic-ischemic encephalopathy. Front Neurol 5: 147, 2014.
23. van Velthoven CT, Kavelaars A and Heijnen CJ: Mesenchymal stem cells as a treatment for neonatal ischemic brain damage. Pediatr Res 71: 474-481, 2012.
24. Zhang X, Zhang Q, Li W, Nie D, Chen W, Xu C, Yi X, Shi J, Tian M, Qin J, *et al*: Therapeutic effect of human umbilical cord mesenchymal stem cells on neonatal rat hypoxic-ischemic encephalopathy. J Neurosci Res 92: 35-45, 2014.
25. Zhou X, Gu J, Gu Y, He M, Bi Y, Chen J and Li T: Human umbilical cord-derived mesenchymal stem cells improve learning and memory function in hypoxic-ischemic brain-damaged rats via an IL-8-mediated secretion mechanism rather than differentiation pattern induction. Cell Physiol Biochem 35: 2383-2401, 2015.
26. Kim YS, Hwang KA, Go RE, Kim CW and Choi KC: Gene therapy strategies using engineered stem cells for treating gynecologic and breast cancer patients (Review). Oncol Rep 33: 2107-2112, 2015.
27. High KA and Roncarolo MG: Gene therapy. N Engl J Med 381: 455-464, 2019.
28. Aiuti A, Slavin S, Aker M, Ficara F, Deola S, Mortellaro A, Morecki S, Andolfi G, Tabucchi A, Carlucci F, *et al*: Correction of ADA-SCID by stem cell gene therapy combined with nonmyeloablative conditioning. Science 296: 2410-2413, 2002.
29. Wang H, Qiu X, Ni P, Qiu X, Lin X, Wu W, Xie L, Lin L, Min J, Lai X, *et al*: Immunological characteristics of human umbilical cord mesenchymal stem cells and the therapeutic effects of their transplantion on hyperglycemia in diabetic rats. Int J Mol Med 33: 263-270, 2014.
30. Kilkenny C, Browne WJ, Cuthill IC, Emerson M and Altman DG: Improving bioscience research reporting: The ARRIVE guidelines for reporting animal research. PLoS Biol 8: e1000412, 2010.

31. Rice JE III, Vannucci RC and Brierley JB: The influence of immaturity on hypoxic-ischemic brain damage in the rat. Ann Neurol 9: 131-141, 1981.
32. Donega V, Nijboer CH, van Tilborg G, Dijkhuizen RM, Kavelaars A and Heijnen CJ: Intranasally administered mesenchymal stem cells promote a regenerative niche for repair of neonatal ischemic brain injury. Exp Neurol 261: 53-64, 2014.
33. Hoogewijs D, Vogler M, Zwenger E, Krull S and Zieseniss A: Oxygen-dependent regulation of aquaporin-3 expression. Hypoxia (Auckl) 4: 91-97, 2016.
34. Livak KJ and Schmittgen TD: Analysis of relative gene expression data using real-time quantitative PCR and the 2(-Delta Delta C(T)) method. Methods 25: 402-408, 2001.
35. Douglas-Escobar M and Weiss MD: Hypoxic-ischemic encephalopathy: A review for the clinician. JAMA Pediatr 169: 397-403, 2015.
36. Burmester T, Ebner B, Weich B and Hankeln T: Cytoglobin: A novel globin type ubiquitously expressed in vertebrate tissues. Mol Biol Evol 19: 416-421, 2002.
37. Ascenzi P, Gustincich S and Marino M: Mammalian nerve globins in search of functions. IUBMB life 66: 268-276, 2014.
38. Amdahl MB, DeMartino AW, Tejero J and Gladwin MT: Cytoglobin at the crossroads of vascular remodeling. Arterioscler Thromb Vasc Biol 37: 1803-1805, 2017.
39. Vinogradov SN and Moens L: Diversity of globin function: Enzymatic, transport, storage, and sensing. J Biol Chem 283: 8773-8777, 2008.
40. Tejero J and Gladwin MT: The globin superfamily: Functions in nitric oxide formation and decay. Biol Chem 395: 631-639, 2014.
41. Hodges NJ, Innocent N, Dhanda S and Graham M: Cellular protection from oxidative DNA damage by over-expression of the novel globin cytoglobin in vitro. Mutagenesis 23: 293-298, 2008.
42. De Beuf A, Hou XH, D'Haese PC and Verhulst A: Epoetin delta reduces oxidative stress in primary human renal tubular cells. J Biomed Biotechnol 2010: 395785, 2010.
43. Lv W, Booz GW, Fan F, Wang Y and Roman RJ: Oxidative stress and renal fibrosis: Recent insights for the development of novel therapeutic strategies. Front Physiol 9: 105, 2018.
44. Lilly B, Dammeyer K, Marosis S, McCallinhart PE, Trask AJ, Lowe M and Sawant D: Endothelial cell-induced cytoglobin expression in vascular smooth muscle cells contributes to modulation of nitric oxide. Vascul Pharmacol 110: 7-15, 2018.
45. Hong SQ, Zhang HT, You J, Zhang MY, Cai YQ, Jiang XD and Xu RX: Comparison of transdifferentiated and untransdifferentiated human umbilical mesenchymal stem cells in rats after traumatic brain injury. Neurochem Res 36: 2391-2400, 2011.
46. Lin YC, Ko TL, Shih YH, Lin MY, Fu TW, Hsiao HS, Hsu JY and Fu YS: Human umbilical mesenchymal stem cells promote recovery after ischemic stroke. Stroke 42: 2045-2053, 2011.
47. van Velthoven CT, Kavelaars A, van Bel F and Heijnen CJ: Nasal administration of stem cells: A promising novel route to treat neonatal ischemic brain damage. Pediatr Res 68: 419-422, 2010.
48. Cunningham CJ, Redondo-Castro E and Allan SM: The therapeutic potential of the mesenchymal stem cell secretome in ischaemic stroke. J Cereb Blood Flow Metab 38: 1276-1292, 2018.
49. Li Y, Cheng Q, Hu G, Deng T, Wang Q, Zhou J and Su X: Extracellular vesicles in mesenchymal stromal cells: A novel therapeutic strategy for stroke. Exp Ther Med 15: 4067-4079, 2018.
50. Gu Y, He M, Zhou X, Liu J, Hou N, Bin T, Zhang Y, Li T and Chen J: Endogenous IL-6 of mesenchymal stem cell improves behavioral outcome of hypoxic-ischemic brain damage neonatal rats by supressing apoptosis in astrocyte. Sci Rep 6: 18587, 2016.
51. Cuadrado A and Nebreda AR: Mechanisms and functions of p38 MAPK signalling. Biochem J 429: 403-417, 2010.
52. Sanchez A, Tripathy D, Yin X, Desobry K, Martinez J, Riley J, Gay D, Luo J and Grammas P: p38 MAPK: A mediator of hypoxia-induced cerebrovascular inflammation. J Alzheimers Dis 32: 587-597, 2012.
53. Cakmak H, Seval-Celik Y, Arlier S, Guzeloglu-Kayisli O, Schatz F, Arici A and Kayisli UA: p38 Mitogen-activated protein kinase is involved in the pathogenesis of endometriosis by modulating inflammation, but not cell survival. Reprod Sci 25: 587-597, 2018.
54. Amir M, Somakala K and Ali S: p38 MAP kinase inhibitors as anti inflammatory agents. Mini Rev Med Chem 13: 2082-2096, 2013.
55. Cheung WD and Hart GW: AMP-activated protein kinase and p38 MAPK activate O-GlcNAcylation of neuronal proteins during glucose deprivation. J Biol Chem 283: 13009-13020, 2008.
56. Park EC and Rongo C: The p38 MAP kinase pathway modulates the hypoxia response and glutamate receptor trafficking in aging neurons. Elife 5: e12010, 2016.
57. Tormos AM, Taléns-Visconti R, Nebreda AR and Sastre J: p38 MAPK: A dual role in hepatocyte proliferation through reactive oxygen species. Free Radic Res 47: 905-916, 2013.
58. Zhang H, Tao L, Jiao X, Gao E, Lopez BL, Christopher TA, Koch W and Ma XL: Nitrative thioredoxin inactivation as a cause of enhanced myocardial ischemia/reperfusion injury in the aging heart. Free Radic Biol Med 43: 39-47, 2007.
59. Xu ZJ, Shu S, Li ZJ, Liu YM, Zhang RY and Zhang Y: Liuwei Dihuang pill treats diabetic nephropathy in rats by inhibiting of TGF-β/SMADS, MAPK, and NF-kB and upregulating expression of cytoglobin in renal tissues. Medicine (Baltimore) 96: e5879, 2017.